Journal of Information Display
Vol. 12, No. 2, June 2011, 101–107

Taylor & Francis
Taylor & Francis Group

Liquid crystal alignment on patterned-alignment films

Jais Bin Lias[a,b*], Thet Naing Oo[c], Tomohiro Yazawa[a], Munehiro Kimura[a] and Tadashi Akahane[a]

[a]*Department of Electrical Engineering, Faculty of Engineering, Nagaoka University of Technology, 1603-1 Kamitomioka, Nagaoka, Niigata 940-2188, Japan;* [b]*Department of Electronic Engineering, Faculty of Electrical and Electronic Engineering, Universiti Tun Hussein Onn Malaysia, 86400, Parit Raja, Batu Pahat, Johor, Malaysia;* [c]*Institute for Materials Chemistry and Engineering, Kyushu University, 6-1 Kasuga-Koen, Kasuga, Fukuoka 816-8580, Japan*

(*Received 7 February 2011; Revised 18 February 2011; Accepted for publication 21 February 2011*)

To come up with a bistable liquid crystal (LC) device using unpolarized UV light, single-step laser patterning on a photoalignment layer using a photomask was proposed to achieve an equilibrium configuration of LC molecules in contact with a periodically patterned substrate. The patterns were formed by stripes of alternating random planar and homeotropic anchoring on a submicrometer scale in the order of 0.5 μm. Two possible configurations of bistable LC cells that can be obtained by combining a micropatterned surface formed with alternating random-planar- and homeotropic-alignment with planar- or homeotropic-alignment surfaces were proposed. The alignment properties of the two proposed models were investigated, along with the microscopic switching behavior of micropatterned nematic LC cells.

Keywords: bistable liquid crystal; random planar alignment; unpolarized UV light; switching behavior

1. Introduction

Most liquid crystal (LC) devices are monostable, with only one possible state in the absence of a field. They require permanent voltage application to maintain another state and frequent image refreshment. This increases the energy consumption and limits the multiplexability. In fact, monostable devices have no intrinsic pixel memory, and to obtain high multiplexing levels, they need an active matrix or other external storage elements. Bistable displays have two (or more) stable states without maintaining an electric field [1,2]. Once displayed, the information is memorized for a long time, ranging from seconds up to years, depending on the application needs. This intrinsic memory is the main advantage of bistable devices. It reduces the power consumption, especially when the application does not require frequent updates. For some mobile applications, such as electronic paper (e-paper), energy saving can be a decisive improvement, increasing the battery lifetime by orders of magnitude.

Flat micropatterned alignment is a novel method for aligning LC [1,3]. Micropatterned surfaces are fabricated by means of a photoalignment technique [4], which generates different surface alignment orientations on a micrometer length scale. This provides unique control of the LC orientation both near the alignment surface and in the bulk of the LC layer. Using micropatterned alignment, a number of new devices have already been realized [3,5,6].

The micropatterned alignment of nematic LCs formed by stripes of alternating random planar and homeotropic alignment was theoretically proposed by Qian and Sheng [7]. They show that novel orientational states and the temperature-dependent tilt angle of the director may be induced in nematic LC by microtextured substrates, i.e., spatially mixed-alignment potentials.

Oo et al. [8–12] and Yazawa et al. [13] proposed single-step laser patterning on a photoalignment layer using a photomask, to achieve an equilibrium configuration of LC molecules in contact with a periodically patterned substrate. The patterns were formed by stripes of alternating planar and homeotropic anchoring. This micropatterned surface provides two equilibrium states with equal energy minima.

The memory effect under the influence of the applied external fields in LC is also an important topic. This type of memory effect maintains the field-induced orientation of LCs caused by external fields after the fields are removed [14–21]. Sato and Wada [14] first reported such memory effect in compensated LCs. They observed that the memory effect depends on the surface conditions of the tin-oxide-coated glass substrate and the applied electric field. Moreover, they found that the temperature range within which the memory effect occurs is inversely proportional to the sample thickness. Therefore, a small sample thickness is needed to achieve the memory effect over a wide temperature range. The other example of these effects

*Corresponding author: Email: jais@stn.nagaokaut.ac.jp

ISSN 1598-0316 print/ISSN 2158-1606 online

DOI: 10.1080/15980316.2011.567826
http://www.informaworld.com

with the application of external fields is the switching of the LC alignment on all bistable surfaces [1,22]. Boyd et al. [1] discovered a new class of nematic LC storage effects based on the elastic and topological bistability of the director orientation, and switching between bistable states was demonstrated using both electric and magnetic fields. They have shown that disclinations, which is anathema to most LC devices, can serve useful functions when properly controlled. Moreover, Dozov and Durand [22] proposed a new kind of passive surface-controlled nematic display with bistable textures. Switching by breaking surface anchoring is very fast and can be controlled by pulses of a few microseconds duration.

In this paper, two kinds of bistable models were demonstrated using a micropatterned surface formed by stripes of alternating random planar and homeotropic alignment. First, the orientation of the bistable models was observed and confirmed under a polarizing optical microscope (POM; Nikon) after being employed with several types of LC substances. Then the alignment properties of the bistable models, such as the twist angle and the pretilt angle, were measured. Lastly, the switching behavior and the memory effect of the bistable model by means of the vertical field effect were observed, and the new states were found to have been memorized after the occurrence of the applied vertical field effect.

2. Bistable switching models

The stripe pattern of the alternating planar- and homeotropic-alignment conditions can induce a first-order phase transition between two bulk orientational states, in which one has the director lying in the *YZ* plane (*YZ* state), where *Z* is normal to the substrate and *Y* is parallel to the stripes, and the other is aligned along the *X* direction (*X* state), as shown schematically in Figure 1(a). This transition can be observed by varying either the temperature (T) or the stripe pattern periodicity (P), or through the application of an electric field (E) in the *Z* direction. In the *YZ* state, the tilt angle of the director (θ), as measured from the substrate, can vary between 7° and 40° as a function of T, P, and E [7].

The bulk orientational state is determined by the competition between the elastic energy in the boundary layer and the surface alignment potential. When P is large, so that the boundary layer elastic energy is smaller than the surface alignment energy, the so-called "*YZ* state" can be obtained as the optimal bulk configuration. As P decreases, the elastic energy in the boundary layer becomes comparable to the surface alignment energy, and a transition may occur. As such, the so-called "*X* state" can be obtained as the optimal bulk configuration. Figure 1(b) shows a schematic illustration of the textured pattern and the director configuration of the *YZ* and *X* states.

Two types of configurations of bistable cells can be obtained by combining a micropatterned surface formed with alternating random-planar- and homeotropic-alignment with either a homogeneous- or a homeotropic-alignment surface. In the twisted-homogeneous model, a micropatterned surface was placed combined with a rubbed polyimide (homogeneous alignment) surface. This was assumed to give two mutually perpendicular homogeneous and twist nematic (TN) states when the *X* and *YZ* states were formed inside the cell. In the bistable hybrid-alignment-nematic (HAN) model, a micropatterned surface was placed combined with a homeotropic surface. This was assumed to have given two mutually perpendicular HAN states when the *X* and *YZ* states were formed inside the cell. The configurations of the bistable LC cells for the twisted-homogeneous and bistable HAN models are shown in Figure 2(a) and (b).

3. Experiments

As a photoalignment layer, vertical polyimide (PI-VA), which originally exhibited homeotropic-alignment, was used. Exposure of the PI-VA film was carried out using one unpolarized beam from a He–Cd laser ($\lambda = 325$ nm, 55.0 mW/cm^2) through a photomask (0.5 μm line and space) incident to the sample from the PI-VA film side, at normal incidence. A depolarizer was used to obtain unpolarized UV light from the polarized UV light source. The exposure time was set at 3 h. Figure 3(a) shows the experimental setup for periodic stripe pattern formation using unpolarized UV light. The pattern was formed by stripes of alternating random planar and homeotropic anchoring, as shown in Figure 3(b).

3.1. Orientation confirmation of the twisted-homogeneous bistable and bistable HAN cells

To observe and confirm the orientation of the twisted-homogeneous bistable and bistable HAN cells, three types

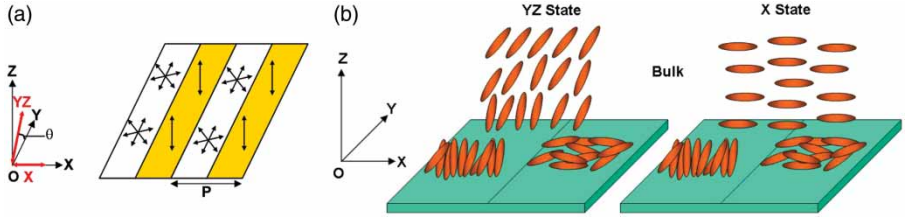

Figure 1. (a) Schematic diagram of the stripe patterns with alternating random-planar- and homeotropic-alignment potentials. (b) Director configuration of the *YZ* and *X* states.

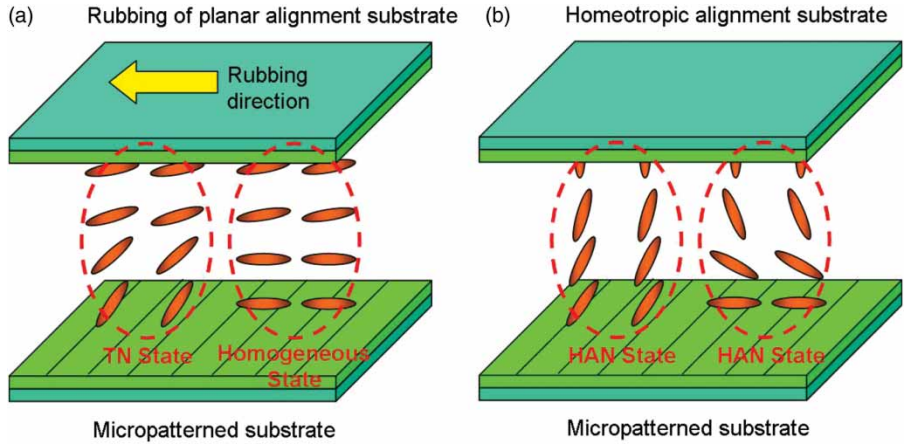

Figure 2. Two types of configurations of the bistable LC cell: (a) twisted-homogeneous bistable mode and (b) bistable hybrid mode.

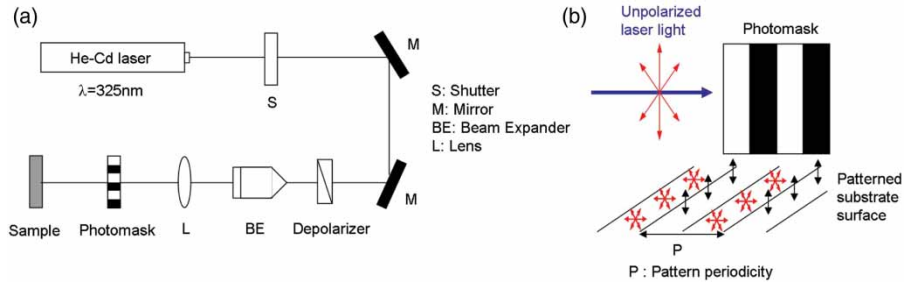

Figure 3. (a) Experimental setup for periodic stripe pattern formation using unpolarized UV light. (b) Schematic illustration of the textured stripe patterns with alternating random-planar- and homeotropic-alignment states after unpolarized UV light exposure.

of nematic liquid crystal (NLC) substances were used. For the twisted-homogeneous bistable cell, the NLC substance with a negative dielectric anisotropy that was used in this experiment was MBBA with a 15 μm nominal cell gap, and the NLC substances with a positive dielectric anisotropy that were used were 5CB (Merck) and ZLI-2293 (Merck) with a 5 μm nominal cell gap. For the bistable HAN cell, the NLC substance with a negative dielectric anisotropy that was used in this experiment was MBBA, and the NLC substance with a positive dielectric anisotropy that was used was ZLI-2293 (Merck). The cells were filled with NLCs by capillary action in the isotropic phase and were gradually cooled to room temperature. The William domains were observed by applying an electric voltage perpendicular to the layer [23,24]. The LC textures for both the twisted-homogeneous bistable and bistable HAN cells were examined under a POM.

3.2. *Measurement of the twisted angle of the twisted-homogeneous bistable cell*

The extinction angle method was used to measure the actual twist angle of the twisted-homogeneous bistable cell [25]. The optical arrangement and the coordinate system of the extinction angle method are shown in Figure 4(a). The alignment and the actual twist angle were determined with a POM between crossed polarizers with white-light illumination [26]. The TN cell was arranged between the polarizer and the analyzer with light incidence. Here, the transmission axis of the polarizer, the transmission axis of the analyzer, and the LC director at the polarizer and analyzer sides are ϕ_p, ϕ_a, n_1, and n_2, respectively. As shown in Figure 4(b), ϕ_p and n_1 were arranged to be parallel to each other while ϕ_a and n_2 were arranged to be perpendicular to each other. At this time, the strength of the light that transmitted the analyzer becomes the smallest. In other words, the linearly polarized light that penetrated the cell and transmitted the polarizer was optically rotated from the direction of n_1 to the direction of n_2 according to the twist of the LC director. The linearly polarized light that was optically rotated was cut off by the analyzer and caused the transmittance to become the smallest. At this time, twist angle Φ_t can be determined using the following equation when the angle formed between ϕ_p and ϕ_a is assumed to be Φ_{pa}:

$$\Phi_t = 90^\circ - \Phi_{pa}. \quad (1)$$

3.3. *Measurement of the pretilt angle of the twisted-homogeneous bistable cell*

The pretilt angle at the *YZ* state (big region) of the patterned substrate was measured by comparing the values of phase difference Δ and angle of amplitude ratio Ψ measured using a transmission spectroscopic ellipsometer (M150, JASCO) [27]. Theoretical calculation was performed using the

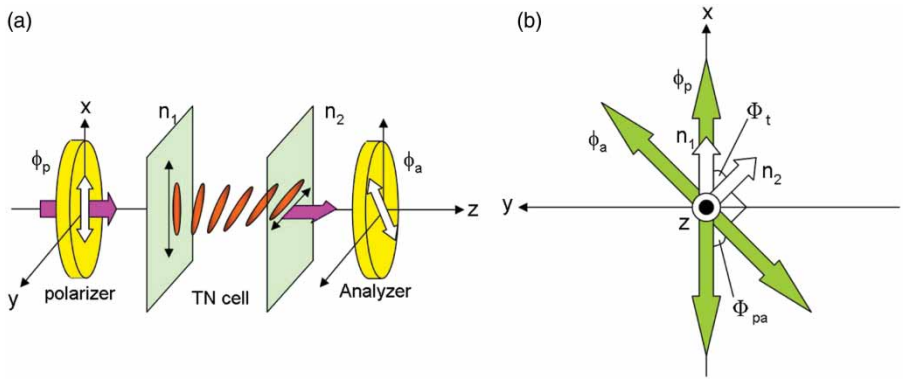

Figure 4. (a) Optical arrangement and coordinate system of the extinction angle method. (b) Polarized light axis related to the director in the extinction angle method.

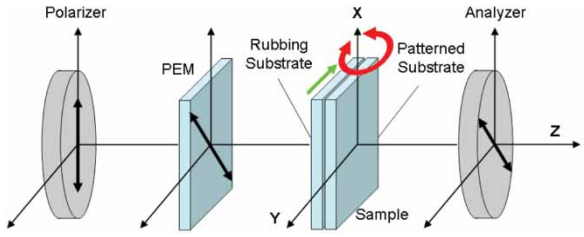

Figure 5. Optical system of the transmission ellipsometer.

Berreman 4 × 4 matrix method [28]. The NLC substance that was used for this experiment was 5CB (5 μm). Figure 5 shows the optical system of the transmission ellipsometer. The incident angles were 0° and 30°. For the theoretical calculation, the twist angle measured through the extinction angle method and the cell gap measured outside the spot area (HAN orientation) through the fitting method were used.

3.4. *Switching experiment of the twisted-homogeneous bistable cell*

A twisted-homogeneous bistable cell filled with 5CB (5 μm) was used for the switching experiment. The pulse voltage was applied, with 100 ms pulse and 80 V voltage amplitude.

4. Results and discussion

4.1. *Orientation confirmation of the twisted-homogeneous bistable and bistable HAN cells*

A micropatterned (random-planar- and homeotropic-alignment) surface was placed combined with a rubbed PI-PA (homogeneous alignment) surface to fabricate a twisted-homogeneous bistable NLC cell, as shown in Figure 2(a). This brought forth the homogeneous and TN states when the *X* and *YZ* states were formed inside the cell, as shown in Figure 6, with the rotation of the analyzer with respect to the polarizer. Figure 6(a), (c), and (d) shows the NLC cells filled with MBBA, 5CB, and ZLI-2293, without electric-field application, respectively. Figure 6(b) shows the NLC cell with electric-field application. The black arrows in Figure 6(b) indicate the LC director when the electric field was applied perpendicular to the layer. Two domains with opposite senses of the twist angle of the LC directors separated by a disclination line were observed, and these were confirmed by the orientation of the William domains. For all the NLC cells, the two states were observed and confirmed. The *YZ* state in the twisted-homogeneous bistable NLC cell was observed to have a bigger region compared with the *X* state.

A micropatterned (random-planar- and homeotropic-alignment) surface was placed combined with a PI-VA (homeotropic-alignment) surface to fabricate a bistable HAN cell. This was assumed to have brought forth two mutually perpendicular HAN states when the *X* and *YZ* states were formed inside the cell, as shown in Figure 7. Figure 7(a) and (c) shows the LC cell filled with MBBA and ZLI-2293 without electric-field application, respectively. Figure 7(b) shows the NLC (MBBA) cell with electric-field application. For both NLC cells, the two HAN states were observed and confirmed under a POM with a crossed polarizer. The disclination line was found between the two HAN states. From the William domains experiment, it was found that the two HAN states were not perpendicular to each other. The *YZ* state in the bistable HAN NLC cell was observed to have a bigger region compared with the *X* state, the same as the twisted-homogeneous bistable cell.

4.2. *Measurement of the twist angle of the twisted-homogeneous bistable cell*

Through the extinction angle method, the actual twist angle of the twisted-homogeneous bistable cell was measured and determined for several samples. Table 1 shows the measurement results of the actual twist angles of MBBA, 5CB, and ZLI-2293. The twisted-homogeneous cell with 5CB was found to have the biggest twist angles within the range of −71 to −78° for the *YZ* state and 58–75° for the *X* state, followed by MBBA with twist angles within the range of −50° to −79° for the *YZ* state and 40–72° for the *X* state,

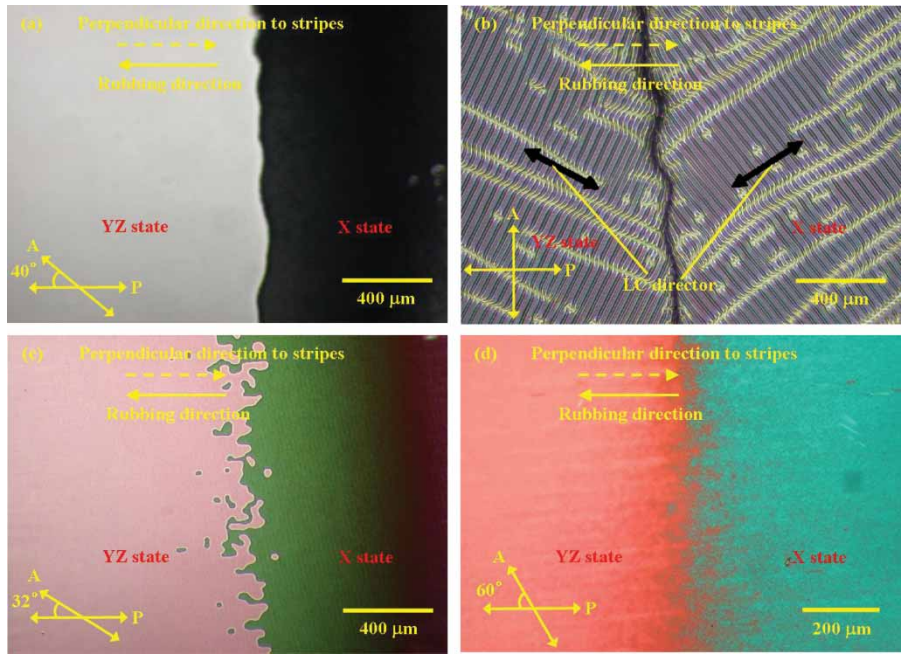

Figure 6. Polarized microphotographs of the twisted-homogeneous bistable cell using different LCs: (a) MBBA without electric-field application; (b) MBBA with electric-field application; (c) 5CB without electric-field application; and (d) ZLI-2293 without electric-field application.

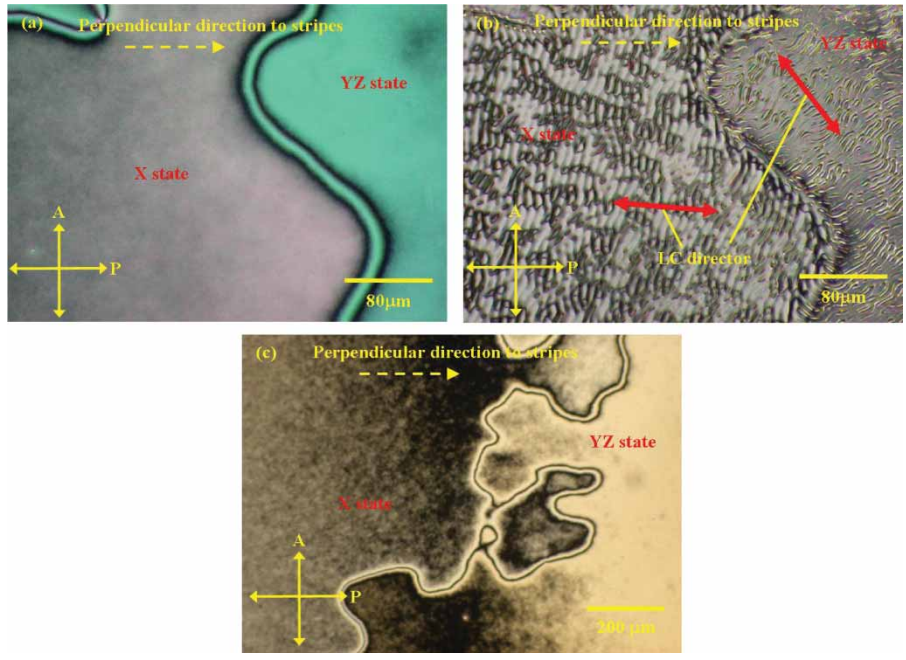

Figure 7. Polarized microphotographs of the bistable HAN cell using different LCs: (a) MBBA without electric-field application; (b) MBBA with electric-field application; and (c) ZLI-2293 without electric-field application.

Table 1. Twist angle measurement results.

Type of NLC	*YZ* state (°)	*X* state (°)
MBBA	−50 to −79	40–72
5CB	−71 to −78	58–75
ZLI-2293	−49 to −52	20–25

and ZLI-2293 with twist angles within the range of −49 to −52° for the *YZ* state and 20–25° for the *X* state. The *YZ* state showed a reverse-twist orientation. The experiment results, in which the twist angles were smaller at the *X* state than at the *YZ* state, are in good agreement, as predicted by Qian and Sheng [7].

4.3. Measurement of the pretilt angle of the twisted-homogeneous bistable cell

By comparing the values of phase difference Δ and angle of amplitude ratio Ψ measured with a transmission spectroscopic ellipsometer, with the theoretical calculation done using the Berreman 4 × 4 matrix method, the pretilt angle at the upper substrate (rubbing substrate) and lower substrate (patterned substrate) were determined to be 2° and 13°, respectively. Figures 8 and 9 show the fitting results of Δ and Ψ at 0° and 30° incidents, respectively.

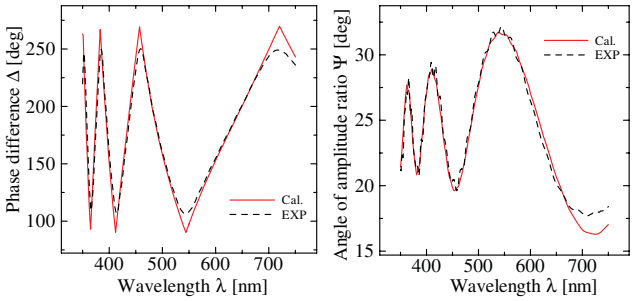

Figure 8. Δ and Ψ on 0° incident.

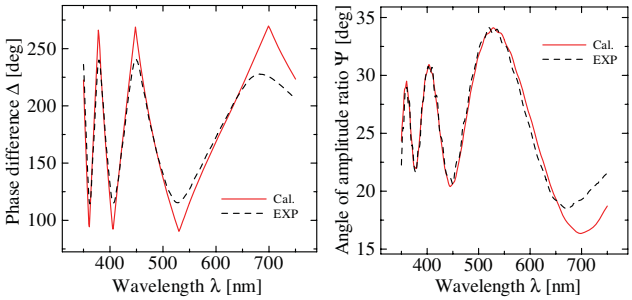

Figure 9. Δ and Ψ on 30° incident.

Therefore, it is understood that the pretilt angle on the patterned-substrate side is comparatively high compared with the rubbing substrate. It is stated in the theory that the *YZ* state has a pretilt angle between 7° and 40° [7]. With this result, it can be said that the big region in the twisted-homogeneous bistable cell is similar to the *YZ* state.

4.4. Switching experiment on the twisted-homogeneous bistable cell

As shown in Figure 10, when the positive square-wave pulse was continuously applied to the twisted-homogeneous bistable cell, a new state was found to have appeared and to have been memorized. It is thought that the new state that appeared was an area of a reverse twist because the color was reversed when the analyzer was rotated. Then, when the negative square-wave pulse was applied to the cell, it was found that the new state was able to be returned to the original state. Therefore, it can be said that the memorized state can be rewritten by changing the polarity of the square-wave pulse. Moreover, the memory state after the application of the switching voltage was maintained for

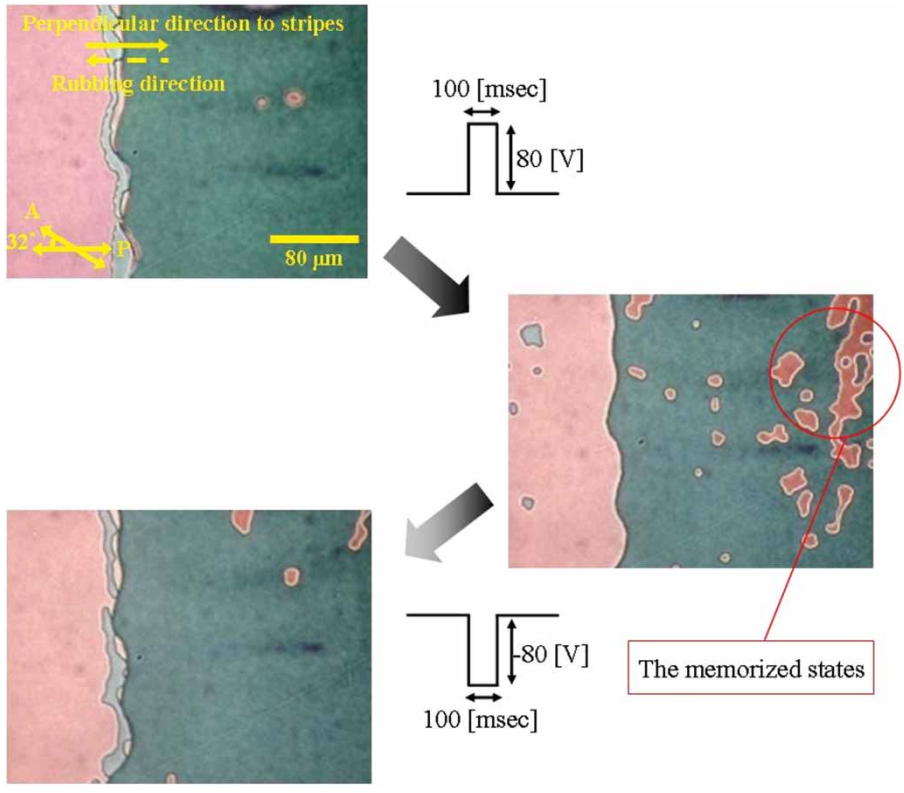

Figure 10. Switching behavior of the twisted-homogeneous bistable cell.

over a month, and it switched to the original state when the pulse of a reverse-polarity electric field was applied.

5. Conclusion

It was found that the two orientational states are quite different from the *X* and *YZ* states as predicted by Qian and Sheng. The two orientational states were confirmed by the orientation of the William domains. Ellipsometric measurements were carried out to determine the deviation from the *X* and *YZ* states. With regard to the twisted-homogeneous bistable cell, the twist angle was measured using the extinction angle method. Moreover, the pretilt angle was estimated by comparing the ellipsometric results of phase difference Δ and angle of amplitude ratio Ψ, with the theoretical calculation done using the Berreman 4×4 matrix method. Furthermore, the pulse voltage was applied to the twisted-homogeneous bistable cell, and the change in the alignment states was observed. The twisted-homogeneous bistable cell showed a peculiar characteristic bistability, and it was found that the two states can be switched using a proper field effect and switching waveforms. The memory state after the application of the switching voltage was maintained for over a month, and it switched to the original state when the pulse of a reverse-polarity electric field was applied. It was thus assumed that the formation of the two bulk orientational states will depend on the degree of depolarization of the laser light, the stripe periodicity, and the effective anchoring strength of the patterned surface.

Acknowledgements

The authors sincerely thank Merck Limited, Japan, and Chisso Petrochemical Corporation for providing them with LC and polyimide materials for this research work.

References

[1] G.D. Boyd, J. Cheng, and P.D.T. Ngo, Appl. Phys. Lett. **36**, 556 (1980).
[2] D.W. Berreman and W.R. Heffner, J. Appl. Phys. **52**, 3032 (1981).
[3] J.H. Kim, M. Yoneya, and H. Yokoyama, Appl. Phys. Lett. **78**, 3055 (2001).
[4] M. O'Neill and S.M. Kelly, J. Phys. D **33**, R67 (2000).
[5] M. Yoneya, J.H. Kim, and H. Yokoyama, Appl. Phys. Lett. **80**, 374 (2002).
[6] B. Wen, J.H. Kim H. Yokoyama, and C. Rosenblatt, Phys. Rev. E **66**, 41502 (2002).
[7] T.Z. Qian and P. Sheng, Phys. Rev. Lett. **77**, 4564 (1996).
[8] T.N. Oo, R. Bansho, N. Tanaka, M. Kimura, and T. Akahane, Jpn. J. Appl. Phys. **45**, 4176 (2006).
[9] T.N. Oo, M. Kimura, and T. Akahane, in *Proc. of the 13th Int. Display Workshops (IDW '06)*, 2006, p. 99.
[10] T.N. Oo, Y. Yasu, M. Kimura, and T. Akahane, Abstr. of the Jpn. Liq. Cryst. Soc. Ann. Mtg., 2006, p. 287.
[11] T.N. Oo, Y. Yasu, M. Kimura, and T. Akahane, Phys. Rev. E **76**, 31705-1 (2007).
[12] T.N. Oo, M. Kimura, and T. Akahane, Adv. Tech. Mat. Mat. Proc. J. **10** (1), 9 (2008).
[13] T. Yazawa, T.N. Oo, M. Kimura, and T. Akahane, in *Proc. of the 14th Int. Display Workshops (IDW '07)* (2007), p. 289.
[14] S. Sato and M. Wada, Jpn. J. Appl. Phys. **11**, 1566 (1980).
[15] J. Cheng and G. D. Boyd, Appl. Phys. Lett. **35**, 444 (1979).
[16] N. Koshida and S. Kikui, Appl. Phys. Lett. **40**, 541 (1982).
[17] T. Nose, S. Masuda, and S. Sato, Jpn. J. Appl. Phys. **30**, 3450 (1991).
[18] R. Yamaguchi and S. Sato, Jpn. J. Appl. Phys. **30**, L616 (1991).
[19] P. Vetter, Y. Ohmura, and T. Uchida, Jpn. J. Appl. Phys. **32**, L1239 (1993).
[20] M. Kawasumi, N. Hasegawa, A. Usuki, and A. Okada, Liq. Cryst. **23**, 769 (1996).
[21] R. Kravchuk and O. Yaroshchuk, Mol. Cryst. Liq. Cryst. **422**, 385 (2004).
[22] I. Dozov and G. Durand, Liq. Cryst. Today **8**, 1 (1998).
[23] C. J. Gerritsma, J.A. Geurst, and A.M.J. Sprujit, Phys. Lett. **43A**, 356 (1973).
[24] S. Frunza, R. Moldovan, T. Beica, M. Giurgea, and D.N. Stoenescu, Europhys. Lett. **20**, 407 (1992).
[25] M. Nobili, R. Barberi, and G. Durand, J. Phys. II France **5**, 531 (1995).
[26] R. Karapinar, M. O'Neil, S.M. Kelly, A.W. Hall, and G.J. Owen, Springer-Verlag, ARI **51**, 61 (1998).
[27] N. Tanaka, M. Kimura, and T. Akahane, Jpn. J. Appl. Phys. **44**, 587 (2005).
[28] D. W. Berreman, J. Opt. Soc. Am. **62**, 502 (1972).